JOURNAL OF QUATERNARY SCIENCE (2010) **25**(2) 146–161

Published online 8 July 2009 in Wiley InterScience
(www.interscience.wiley.com) DOI: 10.1002/jqs.1286

Holocene alpine glaciation inferred from lacustrine sediments on northeastern Baffin Island, Arctic Canada

ELIZABETH K. THOMAS,[1]* JASON SZYMANSKI[2] and JASON P. BRINER[1]
[1] Department of Geology, University at Buffalo, Buffalo, New York, USA
[2] Department of Chemistry and Geosciences, Monroe Community College, Rochester, New York, USA

Thomas, E. K., Szymanski, J. and Briner, J. P. 2010. Holocene alpine glaciation inferred from lacustrine sediments on northeastern Baffin Island, Arctic Canada. *J. Quaternary Sci.*, **Vol. 25** pp. 146–161. ISSN 0267-8179.

Received 12 January 2009; Revised 23 March 2009; Accepted 26 March 2009

ABSTRACT: With accelerated melting of alpine glaciers, understanding the future state of the cryosphere is critical. Because the observational record of glacier response to climate change is short, palaeo-records of glacier change are needed. Using proglacial lake sediments, which contain continuous and datable records of past glacier activity, we investigate Holocene glacier fluctuations on northeastern Baffin Island. Basal radiocarbon ages from three lakes constrain Laurentide Ice Sheet retreat by ca. 10.5 ka. High sedimentation rates (0.03 cm a^{-1}) and continuous minerogenic sedimentation throughout the Holocene in proglacial lakes, in contrast to organic-rich sediments and low sedimentation rates (0.005 cm a^{-1}) in neighbouring non-glacial lakes, suggest that glaciers may have persisted in proglacial lake catchments since regional deglaciation. The presence of varves and relatively high magnetic susceptibility from 10 to 6 ka and since 2 ka in one proglacial lake suggest minimum Holocene glacier extent ca. 6–2 ka. Moraine evidence and proglacial and threshold lake sediments indicate that the maximum Holocene glacier extent occurred during the Little Ice Age. The finding that glaciers likely persisted through the Holocene is surprising, given that regional proxy records reveal summer temperatures several degrees warmer than today, and may be due to shorter ablation seasons and greater accumulation-season precipitation. Copyright © 2009 John Wiley & Sons, Ltd.

Journal of Quaternary Science

KEYWORDS: Holocene; Alpine glaciers; Holocene Thermal Maximum; Baffin Island; lake sediment.

Introduction

Assessing the sensitivity of alpine glaciers to climate warming is a critical priority. Alpine glaciers are currently major contributors to sea-level rise, and this trend is projected to continue throughout the 21st century (Meier *et al.*, 2007). Ice caps in the Canadian Arctic Archipelago are a significant source of eustatic sea-level rise (Abdalati *et al.*, 2004). Although there have been few studies of alpine glaciers in the Canadian Arctic, existing research reveals that most glaciers are retreating rapidly (Paul and Kääb, 2005; Dowdeswell *et al.*, 2007; Anderson *et al.*, 2008). The rapid retreat of glaciers, however, does not coincide with orbital forcing, which is a major driver of climate change during the Holocene (Miller *et al.*, 2005; Briner *et al.*, 2006a). Instead, this retreat is due to rising temperatures that are driven by a combination of anthropogenic and sub-orbital natural forcings (Crowley, 2000; Gillett *et al.*, 2008). Arctic climate and the cryosphere may respond sensitively to these forcings because of strong amplifications associated with albedo feedback mechanisms (Otto-Bliesner *et al.*, 2006; Serreze *et al.*, 2007). Because all indications suggest that marked warming will continue (ACIA, 2005; IPCC, 2007), there is a need to improve our understanding of the sensitivity of arctic glaciers to climate change.

The focus of this study is on Baffin Island, which is the largest island in the Canadian Arctic Archipelago (Fig. 1). Despite significantly less glacier ice on Baffin Island than in the High Canadian Arctic, its glaciers and ice caps are contributing almost half of the sea-level rise attributable to the entire Canadian Arctic (Abdalati *et al.*, 2004). This highlights the sensitivity of Baffin Island to climate warming, in part due to its position near the interchange between the relatively warm, high-salinity West Greenland Current and the cold, low-salinity Baffin Current. Past changes in glacier extent on Baffin Island likely are tied to changes in ocean currents and sea ice extent in Baffin Bay (Dyke *et al.*, 1996a,b). One method used to assess glacier sensitivity to climate change is to reconstruct alpine glacier behaviour during past periods of climate change, in particular, past periods of warmth.

Following retreat of the Laurentide Ice Sheet, summer temperatures warmed significantly throughout the North

*Correspondence to: E. K. Thomas, Department of Geology, University at Buffalo, 411 Cooke Hall, Buffalo, NY 14260, USA.
E-mail: ekthomas@buffalo.edu

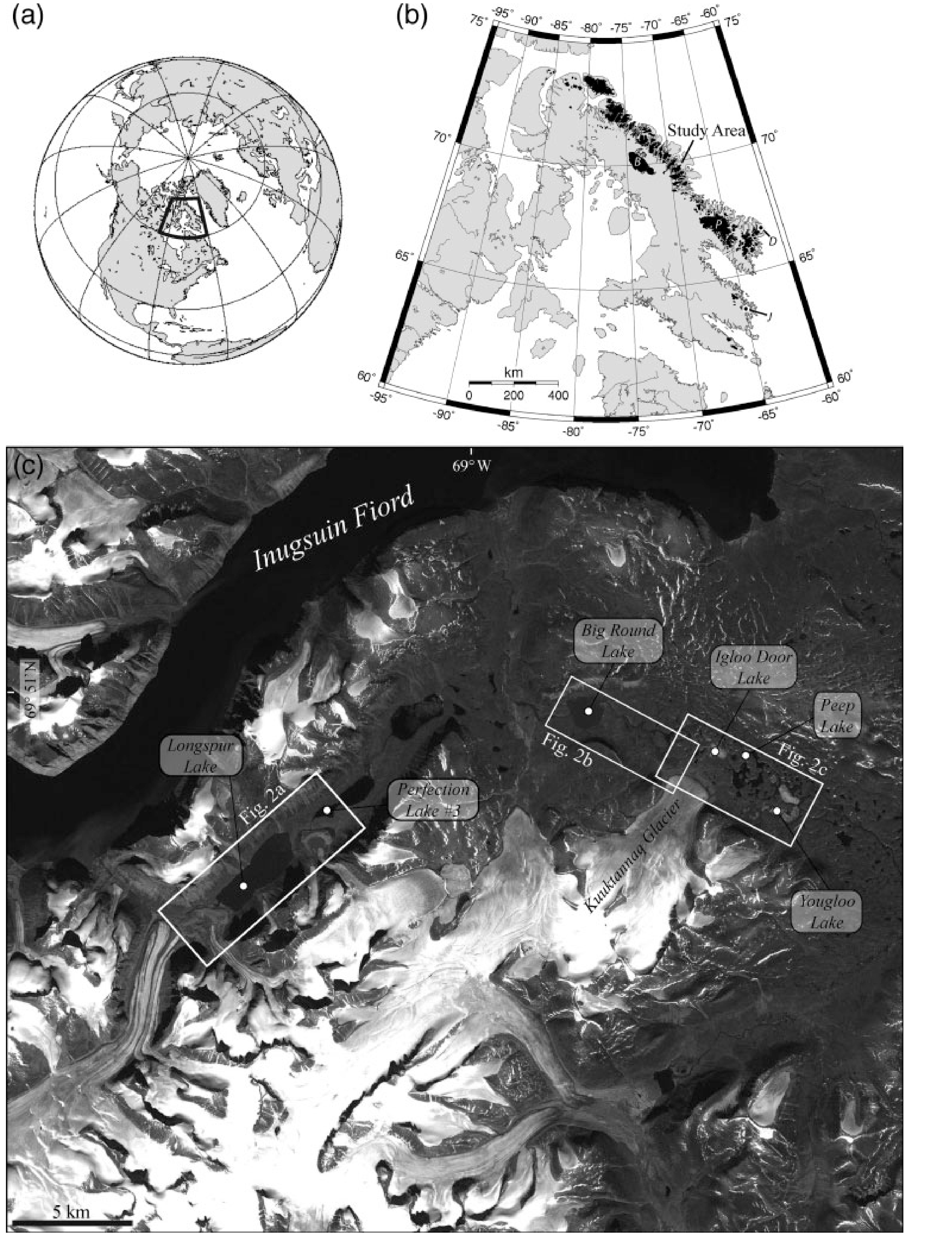

Figure 1 (a) Map of Earth showing location of Baffin Island. (b) Map of Baffin Island showing location of study area and other locations mentioned in the text: B, Barnes Ice Cap; P, Penny Ice Cap; D, Donard Lake; J, Lake Jake. (c) Landsat ETM+ image (bands 1, 2 and 3) of study area, obtained on 30 July 2002. Locations of lakes and Fig. 2(a)–(c) are shown

American Arctic. Holocene climate reconstructions based on various proxies (e.g. pollen, marine molluscs, ice core oxygen isotopes) from the eastern Canadian Arctic indicate mildly (1–2°C) warmer-than-present summer temperatures in the early to middle Holocene (8–4 ka; Kaufman *et al.*, 2004; Kaplan and Wolfe, 2006). On the other hand, several records, including the ice core melt-layer record from the Agassiz Ice Cap on Ellesmere Island and chironomid-inferred summer temperature records from lakes on northeastern Baffin Island, reconstruct arctic summer temperatures up to 5°C warmer than the

20th century from ca. 10 to ca. 7 ka (Fisher *et al.*, 1995; Briner *et al.*, 2006a; Axford *et al.*, 2009). Reconstructions of alpine glaciers through this Holocene Thermal Maximum (HTM) and determining whether mountain glaciers were present at all during the middle Holocene will help evaluate the sensitivity of glaciers to climate change and shed light on their future response to increasing warmth.

The record of Holocene glaciation on Baffin Island reveals widespread glacier expansion in the late Holocene during Neoglaciation, which culminated with maximum glacier extent in recent centuries during the Little Ice Age (Miller, 1973; Davis, 1985; Miller *et al.*, 2005; Briner *et al.*, 2009). However, it remains unclear what state glaciers were in during the HTM before they advanced during Neoglaciation. Small ice caps in north-central Baffin Island were absent in the middle Holocene (Anderson *et al.*, 2008). In contrast, Pleistocene ice has been found at the base of the Barnes and Penny ice caps, indicating that the largest ice caps at present persisted through the HTM (Hooke and Clausen, 1982; Fisher *et al.*, 1998). It remains unclear whether mountain glaciers and small mountain ice caps, which account for the majority of ice on Baffin Island, were present or absent throughout the Holocene. Based on palaeotemperature records, we hypothesise that glaciers were most likely smallest or absent from the landscape during the warm early to middle Holocene.

Because records of glaciation are largely based on moraine records, and because glaciers were most extensive in the late Holocene, knowledge of glaciation from throughout the Holocene is extremely limited. Proglacial lakes, which act as continuous sediment traps and hence record up-valley glacier activity, can provide temporally continuous records of glaciation. There are two proglacial lake records from Baffin Island that reveal glaciation patterns for parts of, but not the entire, Holocene (Moore *et al.*, 2001; Miller *et al.*, 2005). A diamict deposited in Lake Jake at 8.2 ± 0.2 ka is evidence for glacier advance in the early Holocene on southern Baffin Island (Fig. 1; Miller *et al.*, 2005). Donard Lake, a threshold lake that receives glacier meltwater today, but not when glaciers are in reduced states, contains evidence for the initiation of Neoglaciation ca. 6 ka, intensification ca. 2.5 ka, and culmination during the Little Ice Age on southeastern Baffin Island (Moore *et al.*, 2001; Miller *et al.*, 2005). Proglacial lacustrine records of alpine glacier position on Baffin Island that span the entire Holocene, however, are still lacking.

We analysed sediments from proglacial lakes in two adjacent valleys on northeastern Baffin Island to test our hypothesis that glaciers were likely smallest during the warm early to middle Holocene. We analysed sediments from two additional lake types: (1) non-glacial lakes that serve as a control for deciphering the pattern of glacial sedimentation over the Holocene; and (2) threshold lakes that are only proglacial during maximum glacier extent. This work builds on a 1000-year-long late Holocene varve-climate record from a proglacial lake in the study area (Thomas and Briner, 2009).

Setting

Our study lakes are located on northeastern Baffin Island between Inugsuin and McBeth fiords (Fig. 1). The hamlet of Clyde River, 70 km to the north, is the nearest town with a weather station, which has been in operation since 1946. Mean annual temperature at Clyde River is -12.8°C, mean July temperature is 4.4°C and mean annual precipitation is 233 mm a^{-1} (Environment Canada, 2007). Such low amounts of precipitation might suggest that glacier extent is strongly influenced by small changes in precipitation. Because temperatures are generally below freezing from September to late May, ice covers the lakes for ca. 9 months of the year and is $\sim$2 m thick by the end of the winter season. Allochthonous sediment input to the lakes is therefore confined to the ice-free summer months from late June to September.

We recovered lake sediment cores from six lakes that lie on crystalline bedrock in deeply incised valleys (Fig. 1). Perfection Pass (hereafter referred to as Perfection Valley) contains the steepest and highest valley walls, and is the most heavily glaciated. The upper Kuuktannaq River valley (hereafter referred to as Kuuktannaq Valley) is broader and only the southwestern side of the valley is presently glaciated. Both valleys were completely glaciated during the late Pleistocene by the Laurentide Ice Sheet. Recent studies employing cosmogenic exposure dating reveal that deglaciation from the coastal lowlands to the east of the study valleys took place ca. 15 ka, and the mouths of Clyde, Inugsuin and McBeth fiords held outlet glaciers until ca. 11 ka (Briner *et al.*, 2005, 2007; Davis *et al.*, 2006; Bini, 2008). Although there are no cosmogenic exposure ages in the middle reaches of Inugsuin and McBeth fiords, deltas at the fiord heads are as old as ca. 9 ka, suggesting relatively rapid deglaciation of the middle fiord reaches, and hence the study valleys, between ca. 11 and 9 ka. Following deglaciation of the fiords, Laurentide outlet glaciers built moraines and ice-contact marine deltas on eastern Baffin Island between ca. 9.5 and ca. 8 ka, during a period known as the Cockburn Substage (Andrews and Ives, 1978; Briner *et al.*, 2009). Although some mountain glaciers, independent of the Laurentide Ice Sheet, deposited moraines that have been correlated with the Cockburn Substage (Briner *et al.*, 2009), these moraines have not been dated, and mountain glacier advances during the Cockburn Substage have not been identified definitively.

We cored three types of lakes in the Kuuktannaq and Perfection valleys: proglacial, non-glacial and threshold lakes. Two proglacial lakes that we cored are large (>1 km^2 area, >30 m deep) and are fed by a meltwater stream or streams emanating from moraine-forming cirque glaciers and/or alpine ice complexes that compose a large portion ($>20\%$) of the lake catchment. Without knowing the basal thermal regime of glaciers in the study area, we classify each glacier as 'moraine-forming' or 'non-moraine-forming' to provide a qualitative assessment of the amount of sediment that is produced (moraine-forming glaciers likely produce more sediment than non-moraine forming glaciers). In contrast, the two non-glacial lakes that we cored have $<5\%$ non-moraine-forming glacier cover in their catchments. These lakes are small (<0.5 km^2, <11 m deep) and are fed by small, ephemeral streams or are part of a chain of non-glacial lakes. The two threshold lakes that we cored are similar to the non-glacial lakes in size, and for most of the Holocene their catchments are $<25\%$ glacierised by small, non-moraine-forming glaciers. These lakes lie near topographic thresholds that moraine-forming glaciers cross when they advance to their Holocene maximum extents, allowing glacial meltwater and sediment to wash into the lakes.

Methods

Coring

Sediment cores were obtained from six lakes in the Perfection and Kuuktannaq valleys during four field campaigns that took

Table 1 Lake sediment core locations, depths and lengths

Lake name	Lake type	Core name	Latitude (N)	Longitude (W)	Depth (m)	Core type	Core length (cm)
Perfection Lake #4	Proglacial	04PL4-02	69° 47.226′	69° 12.793′	57.35	Long	230
Perfection Lake #4	Proglacial	06PL4-S5	69° 47.324′	69° 12.783′	56.15	Surface	31
Perfection Lake #4	Proglacial	06PL4-P1	69° 48.147′	69° 11.110′	22.80	Long	186
Perfection Lake #4	Proglacial	06PL4-S3	69° 48.141′	69° 11.256′	21.95	Surface	41
Perfection Lake #3	Non-glacial	04PL3-01	69° 48.997′	69° 8.637′	10.90	Long	184
Big Round Lake	Proglacial	06BRD-P1	69° 51.911′	68° 51.571′	36.27	Long	269
Big Round Lake	Proglacial	07BRD-P1	69° 51.910′	68° 51.484′	36.2	Long	379
Big Round Lake	Proglacial	06BRD-S2	69° 51.911′	68° 51.571′	36.27	Surface	34
Peep Lake	Non-glacial	06PEEP-P1	69° 51.163′	68° 40.103′	4.18	Long	64
Igloo Door Lake	Threshold	04IDL-01	69° 51.18′	68° 41.461′	5.63	Long	70
Igloo Door Lake	Threshold	06IDL-S3	69° 51.138′	68° 41.881′	6.35	Surface	63
Igloo Door Lake	Threshold	08IDL-S3	69° 51.206′	68° 41.946′	4.65	Surface	75
Yougloo Lake	Threshold	06UGO-S2	69° 49.851′	68° 36.436′	8.40	Surface	60

place in May of 2004, 2006, 2007 and 2008. A sled-mounted percussion coring system (Nesje, 1992) was used to collect long sediment cores and a Universal Corer (http://www.aquaticresearch.com/) was used to collect surface sediment cores with intact sediment–water interfaces. Table 1 provides details about each core and Fig. 2 shows coring locations. The surface cores were kept vertical and dewatered for several days, and all cores were packed with foam and kept cool until shipment.

Geochronology

We used plutonium ($^{239+240}Pu$) and caesium (^{137}Cs) to date the upper portions of surface cores from two of the lakes. Dried aliquots (0.5 g) of the top 8 cm of the surface core 06BRDS2 (0.5 cm increments, $n = 16$) were analysed at Northern Arizona University for $^{239+240}Pu$ concentrations using inductively coupled plasma mass spectrometry (ICP-MS) following the

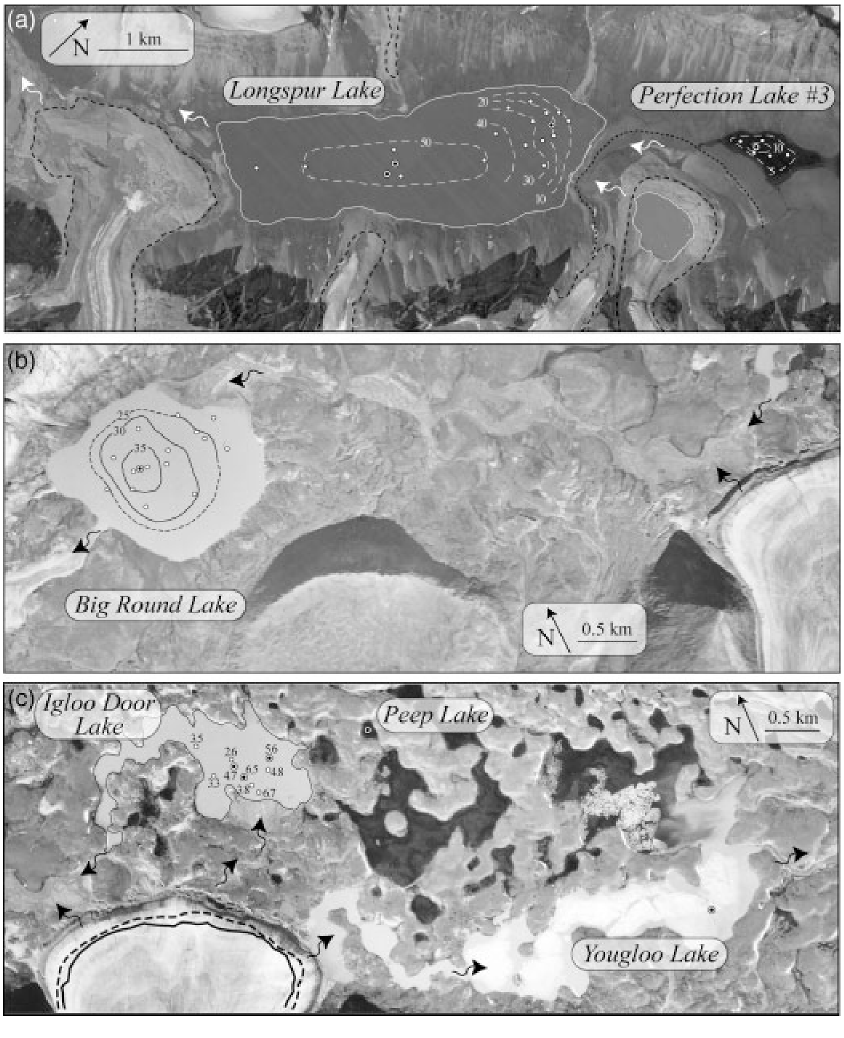

Figure 2 Maps of study locations showing lake bathymetry (lines and white dots), moraine crests, core locations (black and white dots) and inflow/outflow streams. (a) Google Earth image of Perfection Valley. (b) 1 September 1960 vertical aerial photograph (reproduced with the permission of Natural Resources Canada 2008, courtesy of the National Air Photo Library) showing Big Round Lake and its inflow stream from the Kuuktannaq Glacier. (c) 1 September 1960 vertical aerial photograph showing the Kuuktannaq Valley with Igloo Door, Peep, and Yougloo lakes, and the Kuuktannaq Glacier with 1990 (dotted line) and 2000 (solid line) extents, mapped using Landsat TM and ETM+ images

DOI: 10.1002/jqs

methods of Ketterer *et al.* (2004). Dried aliquots (2–3 g) of surface core 06PL4-S5 (~2 cm increments, $n = 12$) were analysed for ^{137}Cs using thermal ionisation mass spectrometry (TIMS) following the methods of Chen *et al.* (2008).

Dating arctic lake sediments using radiocarbon is complicated (Wolfe *et al.*, 2004). Low within-lake primary productivity, particularly in deep, turbid proglacial lakes, results in little autochthonous datable material. A low rate of terrestrial plant decomposition in the watershed results in radiocarbon-depleted organic material in soils, and consequently radiocarbon-depleted pools of dissolved organic carbon and lake sediment (Abbott and Stafford, 1996). Terrestrial macrofossils and bulk sediment are therefore potentially older than their deposition age. The lakes in this study are underlain by Precambrian crystalline terrain of the Canadian Shield, and consequently there is little or no hard-water effect. Miller *et al.* (1999) demonstrated that aquatic organisms utilising dissolved inorganic carbon as their primary carbon source have the same radiocarbon activity as the contemporaneous atmosphere, and aquatic macrofossils were therefore the primary target for dating in this study. Where aquatic macrofossils were not available, we dated either humic acid extracts from bulk sediment or terrestrial plant macrofossils (Table 2). Samples for radiocarbon dating were picked, washed and placed in sterilised glass vials at the University at Buffalo Paleoclimate Lab. Fourteen samples were submitted for preparation at the INSTAAR Laboratory for AMS Radiocarbon Preparation and Research at the University of Colorado and measurement at the W. M. Keck Carbon Cycle AMS Facility at the University of California, Irvine; 17 were submitted for preparation and measurement at the Accelerator Mass Spectrometry Laboratory at the University of Arizona (Table 2).

Physical properties

Magnetic susceptibility (MS) was measured every 0.5 cm on the split core faces using a Bartington MS2E surface scanning sensor connected to a Bartington MS2 magnetic susceptibility meter. Loss-on-ignition at 550°C (LOI) was measured on an aliquot (~100 mg) of subsamples collected at 0.5–1.0 cm increments. Grain size was measured at 1 cm increments on a Beckman Coulter Model LS 230 laser particle size analyser after acid and base pre-treatments to remove biogenic components (aquatic and terrestrial macrofossils, and diatoms).

Lamination analysis

Two surface cores and a section of one long core were made into thin sections following methods similar to Lamoureux (1994) and Francus and Asikainen (2001). The thin sections were scanned using a transparency scanner at 1600 dpi (e.g. Lamoureux and Gilbert, 2004). Laminated couplets were

Table 2 Radiocarbon ages used in this study

Core	Depth (cm)	Material dated	Fraction modern	Radiocarbon age (^{14}C a BP)	Calibrated age (cal. a BP $\pm 1\sigma$)[a]	$\delta^{13}C$ (‰ PDB)	Lab number[b]
04PL4-02	18	Terrestrial plant fragments	0.9417 ± 0.0014	480 ± 15	520 ± 10	−26.9	CURL8926
04PL4-02	93	Terrestrial plant fragments	0.8999 ± 0.0014	845 ± 15	750 ± 20	−24.4	CURL8213
04PL4-02	115	Terrestrial plant fragments	0.7440 ± 0.0014	2375 ± 15	2360 ± 10	−21.7	CURL8930
04PL4-02	145.5	Terrestrial plant fragments	0.6900 ± 0.0330	2980 ± 380	3190 ± 460	−27.1	AA71100
04PL4-02	167.5	Terrestrial plant fragments	0.7978 ± 0.0035	1815 ± 40	1780 ± 30	−30.3	AA71099
04PL4-02	185	Terrestrial plant fragments	0.7186 ± 0.0012	2655 ± 15	2760 ± 10	−22.0	CURL8212
04PL4-02	218	Terrestrial plant fragments	0.6677 ± 0.0060	3245 ± 70	3480 ± 80	−29.5	AA60647
06PL4-P1	9	Terrestrial plant fragments	0.9850 ± 0.0058	120 ± 50	130 ± 130	−25.7	AA71097
06PL4-P1	40	Terrestrial plant fragments	0.8661 ± 0.0037	1155 ± 30	1080 ± 90	−24.0	AA71098
06PL4-P1	71	Terrestrial plant fragments	0.7297 ± 0.0011	2530 ± 15	2640 ± 90	−29.2	CURL8836
06PL4-P1	177	Terrestrial plant fragments	0.3739 ± 0.0009	7905 ± 20	8690 ± 60	−20.7	CURL8928
04PL3-01	107	Terrestrial plant fragments	0.3193 ± 0.0010	9170 ± 25	10310 ± 60	−26.6	CURL8272
06BRD-P1	28.5	Aquatic plant fragments	0.9029 ± 0.0015	820 ± 15	720 ± 20	−14.6	CURL8932
06BRD-P1	57	Insect pieces, terrestrial and aquatic plant fragments	0.8486 ± 0.0063	1320 ± 60	1240 ± 60	−23.2	AA71101
06BRD-P1	77.5	Aquatic and terrestrial plant fragments	0.7231 ± 0.0012	2605 ± 15	2750 ± 10	−21.1	CURL9416
06BRD-P1	166	Aquatic plant fragments	0.5713 ± 0.0040	4500 ± 60	5170 ± 120	−23.9	AA71102
06BRD-P1	243.5	Aquatic and terrestrial plant fragments	0.4380 ± 0.0012	6630 ± 25	7530 ± 40	−20.1	CURL8931
07BRD-P1	298.5	Aquatic plant fragments	0.3680 ± 0.0006	8030 ± 15	8910 ± 100	−22.6	CURL9409
06PEEP-P1	1	Aquatic plant fragments	0.8700 ± 0.0120	1120 ± 110	1080 ± 90	−25.2	AA71106
06PEEP-P1	1	Bulk sediment	0.7472 ± 0.0067	2340 ± 70	2420 ± 90	−28.0	AA71107
06PEEP-P1	14	Aquatic plant fragments	0.5640 ± 0.0080	4600 ± 110	5260 ± 200	−25.5	AA71108
06PEEP-P1	14	Bulk sediment	0.5993 ± 0.0046	4110 ± 60	4670 ± 140	−27.0	AA71109
06PEEP-P1	64	Aquatic plant fragments	0.3162 ± 0.0022	9250 ± 55	10400 ± 110	−28.9	AA71103
04IDL-01	46.25	Aquatic plant fragments	0.3283 ± 0.0008	8945 ± 20	10080 ± 120	−30.5	CURL10082
06IDL-S3	8.5	Bulk sediment	0.8666 ± 0.0062	1150 ± 60	1070 ± 90	−29.3	AA71113
06IDL-S3	15	Bulk sediment	0.8174 ± 0.0047	1620 ± 50	1490 ± 70	−26.1	AA71114
06IDL-S3	55	Aquatic plant fragments	0.3788 ± 0.0038	7800 ± 80	8620 ± 170	−24.4	AA71104
08IDL-S3	73.7	Aquatic plant fragments	0.3560 ± 0.0007	8295 ± 20	9340 ± 60	−30.5	CURL10095
06UGO-S2	2.5	Bulk sediment	0.8022 ± 0.0072	1770 ± 70	1710 ± 100	−28.5	AA71115
06UGO-S2	36	Aquatic plant fragments	0.3237 ± 0.0038	9060 ± 95	10180 ± 220	−28.5	AA71105

[a] Calibrated using CALIB 5.0.2.
[b] CURL numbers from INSTAAR Laboratory for AMS Radiocarbon Preparation and Research; AA numbers from Accelerator Mass Spectrometry Laboratory at the University of Arizona.

identified, marked and counted in Adobe Illustrator and lamination thicknesses were measured perpendicular to the laminations using ImageJ software. Varve identification and chronology were accomplished using the $^{239+240}$Pu and ^{137}Cs profiles (Szymanski, 2008; Thomas and Briner, 2009).

Glacial and non-glacial sediment

Because the conclusions of this study depend on the interpretation of lake sediment stratigraphy, here we outline the types of sediment found and our general interpretations thereof. Previous studies of lake sediments on Baffin Island determined that lakes with no modern glacial input typically contain olive-brown, organic-rich (>10% LOI) sediment with a minor minerogenic component (MS $\approx$ 0 cgs units; Michelutti *et al.*, 2005; Briner *et al.*, 2006a). In this study, sediment cores from the two non-glacial lakes also exhibit these characteristics (see below). Sediment cores from the two threshold lakes, which only receive glacial meltwater when moraine-forming glaciers cross into their catchments during periods of maximum ice extent, contain 1–15 cm of laminated silt or silty organic sediment (<3% LOI, MS $\approx$ 10–100 cgs units) overlying olive-brown, organic-rich sediment typical of non-glacial lakes (see below). Sediment cores from the two proglacial lakes that receive meltwater from at least one moraine-forming glacier today are much longer than those obtained from the non-glacial and threshold lakes (i.e. higher sedimentation rate) and they contain laminated silt punctuated by sand layers (see below). Laminated silt at the surface of both lake sediment sections is deposited annually, i.e. varved (Szymanski, 2008; Thomas and Briner, 2009). LOI is low (<5%) and MS tends to be high (>100 cgs units) in these sediments.

We acknowledge that there are processes other than glacial by which laminated minerogenic sediments are deposited into lakes. However, we interpret thinly laminated silt-rich sediments punctuated by sand layers to be *most likely* glacial in origin based on two lines of reasoning. First, in the two proglacial lakes that we cored, modern sediments are glacial in origin, and similar facies deposited earlier in the Holocene are likely also glacial. Second, non-glacial lakes adjacent to the proglacial lakes in our study area, with similar catchment morphology, do not contain laminated, minerogenic sediment but instead contain organic-rich sediment throughout (see below). Thus, if at any time during the Holocene glaciers were absent in the proglacial lake catchments, the sediments would most likely exhibit properties similar to those found in neighbouring non-glacial lakes. We interpret Holocene glaciation from lake sediments on this basis, but acknowledge that there are alternative processes that lead to laminated minerogenic lake sediment.

Lacustrine archives in Perfection Valley

Longspur Lake

Longspur Lake is a proglacial lake with a 93.5 km^2 catchment (69° 48′ N, 69° 12′ W) and receives meltwater directly from five moraine-forming glaciers that terminate ~1 km or less from the lake shoreline (Fig. 2(a)). The 4.9 km^2 lake is bounded by 900 m high valley walls along the long axis and by moraines at both ends. The largest inflow stream, at the northeastern end of Longspur Lake, drains three non-glacial lakes as well as a large outlet glacier that lies east of the lake (Fig. 1). Longspur Lake also received sediment from a large glacier at the southwestern end of the lake when this glacier was more extensive. During the peak of Neoglaciation, all six of the glaciers around Longspur Lake deposited moraines within 1 km of the lake, but only one of them may have breached the lake's shoreline. Limited bathymetry from the lake indicates that it has a single basin that reaches ~57 m depth near the lake's centre (Fig. 2(a)). We collected long cores and adjacent surface cores from two different locations within Longspur Lake: one in the central, deepest portion of the lake and one in a shallower site closer to the eastern end (Fig. 2(a)).

Deep core site

A long core/surface core pair was retrieved from near the centre of Longspur Lake, 900 m from the crest of a Little Ice Age moraine deposited by a cirque glacier on the southeastern side of the lake (Fig. 2(a)). The long core (04PL4-02; 57.35 m depth; 69° 47.226′ N, 69° 12.793′ W) is 230 cm long (Table 1 and Fig. 3). The upper 29 cm of this core is composed of silt and sand, which was disturbed during retrieval and transport. A massive coarse sand unit extends from 29 to 65 cm depth. Below 65 cm, core 04PL4-02 is characterised by millimetre-scale silt laminations interrupted by fining-upwards sand sequences ~1–15 cm thick that are probably turbidity flow deposits. The MS profile reflects the sedimentation pattern in this core: high MS where there are coarse layers and lower MS in between. No aquatic macrofossils were found in this core; terrestrial macrofossils from seven turbidite layers were used for radiocarbon dating (Table 2).

We collected a 31 cm long surface core (06PL4-S5; 56.15 m depth; 69° 47.324′ N, 69° 12.783′ W; Table 1 and Fig. 3) that contains intact sediments from the interval in the long core that was disturbed. The surface core has millimetre-scale silt laminations to 27 cm depth. ^{137}Cs analyses support that the laminations are varves, which extend back to AD 1788 (Szymanski, 2008). At 28 cm in 06PL4-S5 is a sand layer that we interpret as the same sand layer from 29 to 65 cm depth in the adjacent long core. As in the long core, the MS profile of the surface core reflects the sedimentology: high and low MS represent sand layers and finer-grained sediment, respectively.

A composite chronology for the deep basin site was developed using radiocarbon ages from the long core and the surface core varve chronology, fitted to a polynomial curve (Fig. 4(a)). Establishing the age–depth model is difficult because all radiocarbon ages are from terrestrial macrofossils and there is some scatter in the ages. However, after removing three ages which were old with respect to the rest of the chronology, shown in Fig. 4(a), the age–depth model intersects the surface and provides plausible sedimentation rates. Based on the chronology presented in Fig. 4(a), this record begins ca. 4360 cal. a BP. Sedimentation rates increased steadily from 0.02 cm a^{-1} in the middle Holocene to ~0.12 cm a^{-1} in recent centuries.

Shallow core site

The second long core/surface core pair retrieved from Longspur Lake is located ~0.5 km northwest of the main inflow stream (Fig. 2(a)). The long core (06PL4-P1; 22.80 m depth; 69° 48.147′ N, 69° 11.110′ W) is 186 cm long (Table 1 and Fig. 5). The upper 77 cm of this core are composed of weakly laminated silt punctuated every few centimetres with millimetre-scale sand stringers, some of which contain macrofossils. There are two coarse-grained, massive sand layers at 42–47 cm and 77–95 cm. Below 95 cm the sediment is a mixture of

DOI: 10.1002/jqs

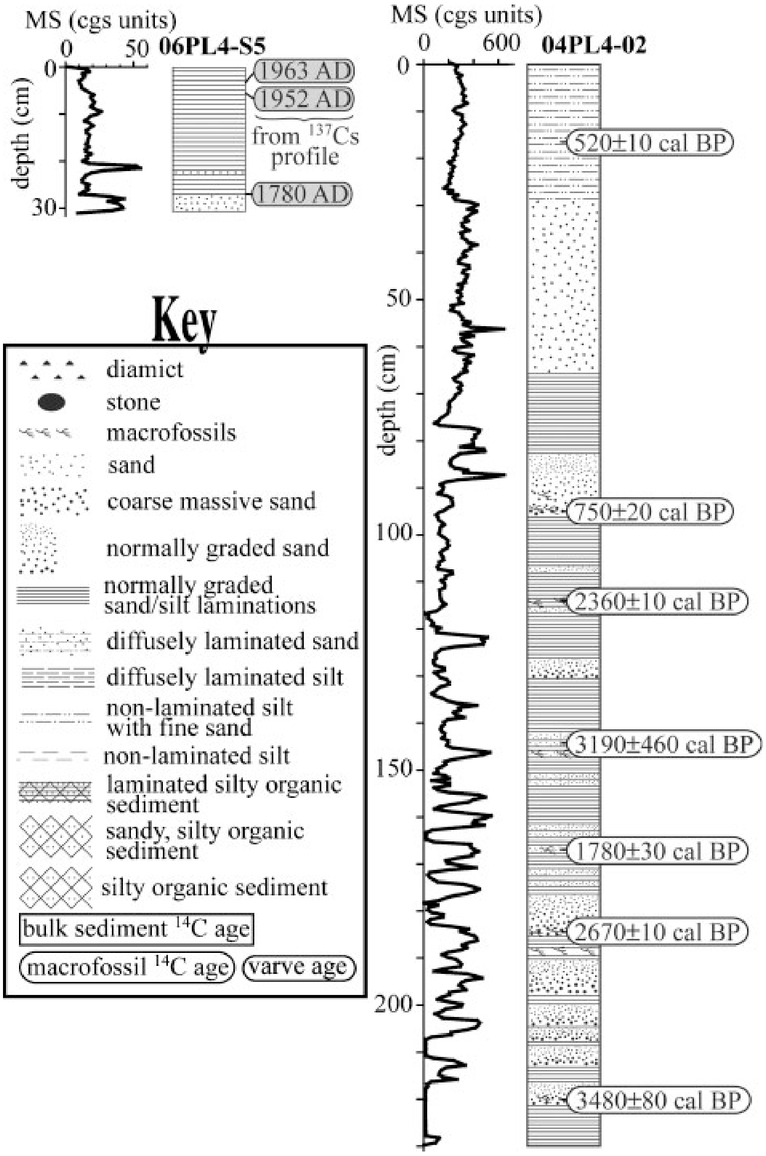

Figure 3 Core logs from the deep core site of Longspur Lake, with age controls. The key is the same for all core log figures

coarsely laminated sand and silt. Macrofossils are much less abundant in the lower portion of the core.

The surface core, retrieved with an intact sediment–water interface, (06PL4-S3; 21.95 m depth; 69° 48.141′ N, 69° 11.256′ W) is 41 cm long (Table 1 and Fig. 5). It is similar to the upper portion of the long core: weakly laminated silt interspersed with sand stringers and some macrofossils. The upper ~3 cm of the surface core is laminated silt. We used the MS and LOI profiles to correlate the surface and long cores, and create a composite stratigraphy for the core site. The MS profile is high where there are sand layers. LOI is ~6% below 95 cm and then decreases in a stepwise fashion to <2% above 95 cm. LOI is higher where there are sand layers with abundant macrofossils.

We measured sediment grain size in cores from this shallow site because of its proximity to the shore and to the main, glacier-dominated inflow stream. Changes in either the energy or sediment load of the inflow stream or the proximity of this core site to the shore could cause the sediment grain size to shift. Grain size, measured on both cores at 1 cm intervals (Fig. 5), reveals sediment below 95 cm consisting of an average of 32% sand, 63% silt and 5% clay. Small sand layers visible in this lower portion of the core stand out as brief 1–3 cm intervals of coarser grain size. Above 77 cm, sediments are much finer, with an average of 2% sand, 82% silt and 16% clay. The sand layer at 77–95 cm is 72% sand, with only 26% silt and 2% clay (Fig. 5). In contrast, the upper sand layer at 42–47 cm has roughly equivalent sand and silt fractions, 45% sand and 52% silt, with 3% clay. Within each of these units, grain size remains relatively constant. The significant change from sand-and-silt-dominated sediment below 77 cm to silt-dominated sediment above 77 cm may be indicative of dramatic shifts in the energy regime at this core site.

As in the deep basin, no aquatic macrofossils were found; terrestrial plant fragments from four intervals were used for radiocarbon dating (Table 2). A chronology was developed by fitting a polynomial curve to the four radiocarbon-dated intervals and assuming that the top of the surface core was deposited in AD 2006 (Fig. 4(b)). The two cores were spliced using grain size, LOI and MS, and approximately 7 cm was lost from the top of the long core. The age at 9 cm depth in the long core (120 ± 50 ^{14}C a BP; 130 ± 130 cal. a BP) suggests that this sample (and therefore potentially other samples) was transported to and deposited on the lake bottom without being retained on the landscape for any substantial amount of time. Based on the age model, the record from the shallow core site extends to 9200 cal. a BP. Similar to the deep core site, sedimentation rate is higher in the late Holocene (up to 0.50 cm a^{-1}), and lower in the early and middle Holocene (0.02 cm a^{-1}).

DOI: 10.1002/jqs

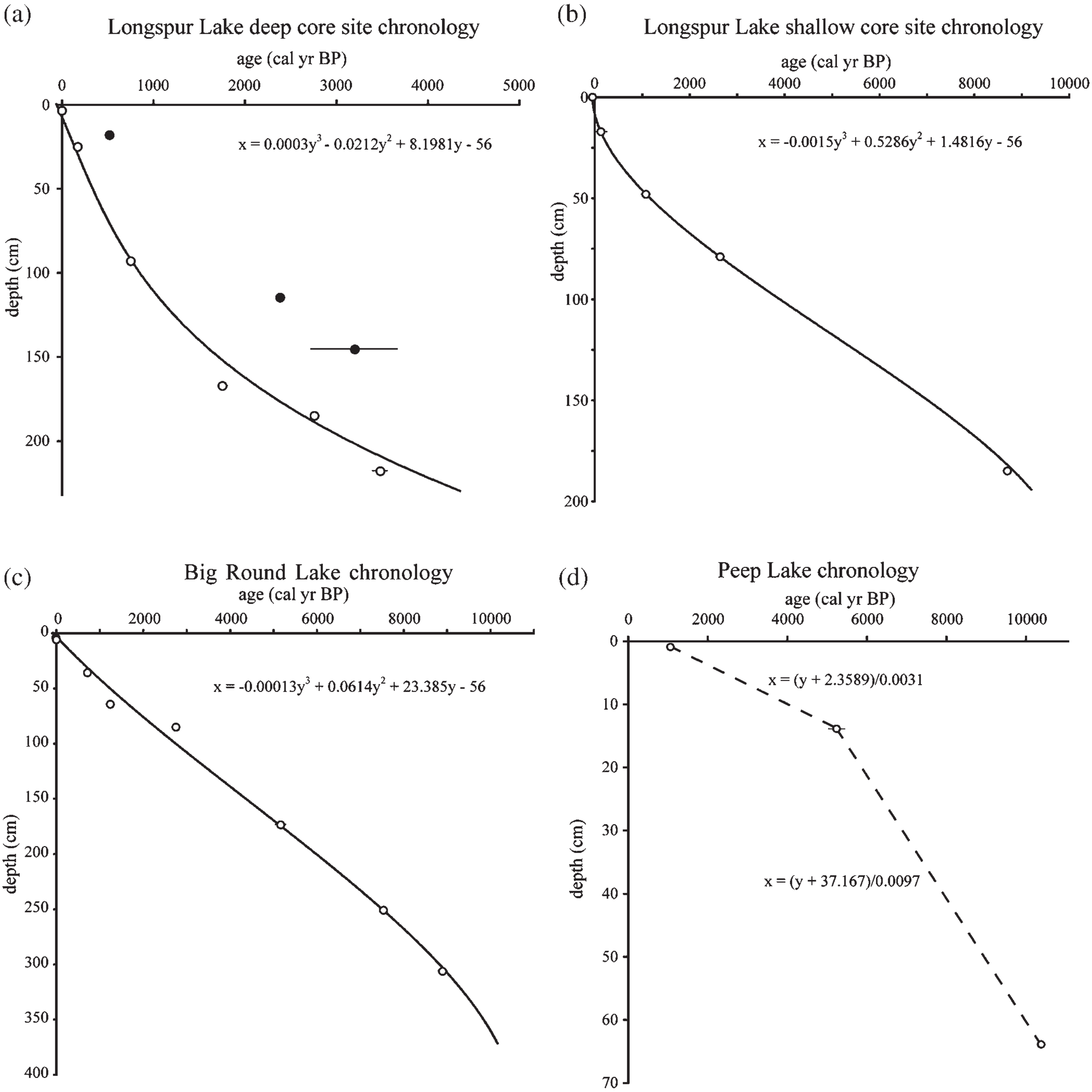

Figure 4 Age–depth profiles for: (a) the deep core site of Longspur Lake; (b) the shallow core site of Longspur Lake; (c) Big Round Lake; and (d) Peep Lake. Solid data points are old outliers that were not used to calculate the age–depth model. Error bars are plotted; most are smaller than the data points

Interpretation of glacier extent in the Longspur Lake catchment

The coarse sand unit from 29 to 65 cm in the deep basin requires very high-energy transport. The most likely source for such a deposit is the cirque glacier on the southeastern side of the lake that deposited a moraine along the shoreline ~700 m from the deep basin core site. While the glacier was at its maximum extent and the moraine was being built, turbidity flows probably originated from the steep moraine front and carried coarse sediment into the Longspur Lake basin. Although the bottom contact of the sand unit is not dated, extrapolation of the sedimentation rate based on four radiocarbon ages in lower sediments yields an age of approximately 470 cal. a BP. The top of the sand layer can be dated via varve counting in the surface core 06PL4-S5, which terminates in sand at 28 cm depth. The sand is at a similar depth to the upper contact of sand in 04PL4-02 (29 cm); the sand at the base of the surface core precedes varve year 171 cal. a BP. Thus, the sandy sediments were most likely deposited between ca. AD 1500 and ca. 1800.

The shallow core site contains evidence of a dramatic shift in energy regime. A ~15 cm thick layer of sand-rich sediment that dates to ca. 3.0 ka is followed by a virtual disappearance of sand and subsequent increases of silt and clay percentages at ca. 2.5 ka. It is difficult to know exactly why this significant change in sedimentation occurred, but one possibility is that it relates to a rise in lake level as glaciers dammed the lake's outlet. At present, voluminous moraines deposited by a long outlet glacier dam Longspur Lake's outlet (Figs. 1(c) and 2(a)). Perhaps the glacier neared its Little Ice Age margin as early as ca. 3 ka and dammed the Lake Longspur outlet, raising lake level and causing a sudden fining of sediments at the core site.

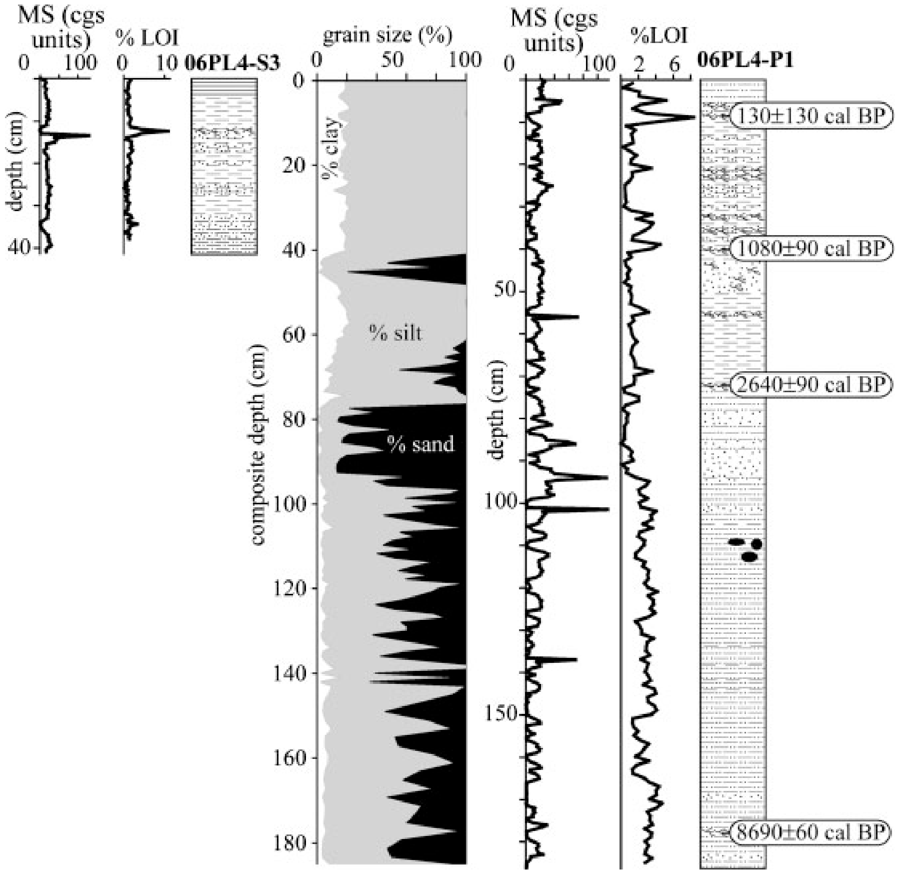

Figure 5 Core logs from the shallow core site of Longspur Lake, with age controls. Grain size for both cores is plotted as composite depth. See Fig. 3 for key

Perfection Lake #3

Perfection Lake #3 (informal name) is third in the chain of three non-glacial lakes that flow into Longspur Lake. Meltwater from two small glaciers feeds directly into Perfection Lake #3. Unlike the glaciers that surround Longspur Lake, these glaciers are non-moraine forming. Perfection Lake #3's area is 0.4 km^2 with a 50.1 km^2 catchment. The lake is dammed by a subdued moraine with mature vegetation cover that pre-dates Neoglaciation (Fig. 2(a)). The single basin in Perfection Lake #3 is deepest (10.90 m) near the centre of the lake (Fig. 2(a)). We retrieved a 184 cm long core from the deep basin (04PL3-01; 69° 48.997′ N, 69° 8.637′ W; Table 1 and Fig. 6). The upper 107 cm of this core is composed of organic-rich sediment. MS decreases and LOI increases slowly from 107 cm to the surface. An aquatic macrofossil from the base of this unit (107 cm) was dated to 10 310 ± 60 cal. a BP. This translates to an average Holocene sedimentation rate of 0.01 cm a^{-1}.

There are two distinct units below the organic-rich unit: a sandy diamicton extends from 107 to 147 cm and a pebble- and cobble-rich diamicton extends from 147 cm to the base of the core. MS is high throughout these two units. LOI was measured only in the upper few centimetres of the sandy diamicton, and was low (<1%).

Interpretation of glaciation based on Perfection Lake #3 sediments

Throughout the Holocene, non-glacial Perfection Lake #3 experienced lower sedimentation rates than neighbouring proglacial Longspur Lake. There are no visible minerogenic laminations and there is very little minerogenic input to Perfection Lake #3 compared to Longspur Lake. This suggests that, while aquatic productivity dominated sedimentation in Perfection Lake #3, Longspur Lake was receiving minerogenic sediment throughout the Holocene, implying that alpine glaciers persisted through the early and middle Holocene.

Perfection Lake #3 also provides an age constraint on the pre-Neoglacial moraine that dams the lake. The radiocarbon age at the base of the organic lacustrine sediments indicates that organic sedimentation began in Perfection Lake #3 around 10.3 cal. ka BP, and continued to the present without interruption. The pre-Neoglacial moraine therefore must have been deposited prior to 10.3 cal. ka BP, and does not correlate with the Cockburn Substage of the Laurentide Ice Sheet.

Lacustrine archives in Kuuktannaq Valley

Big Round Lake

Big Round Lake (informal name) is a proglacial lake with a 65.0 km^2 catchment and receives meltwater directly from the Kuuktannaq Glacier, a moraine-forming outlet glacier, via a 5 km long stream (Fig. 2(b)). The 1.3 km^2 lake lies between a 150 m high hill to the south and 500 m high cliffs to the north. Big Round Lake has one outflow that drains into Inugsuin Fiord (Fig. 2(b)). The single basin is 36 m deep at the deepest point near the lake's centre. We collected two long percussion cores and an adjacent surface core from the central, deepest portion of the lake.

The first long core (06BRD-P1; 36.27 m depth; 69° 51.911′ N, 68° 51.571′ W) is 269 cm long. The second long core

DOI: 10.1002/jqs

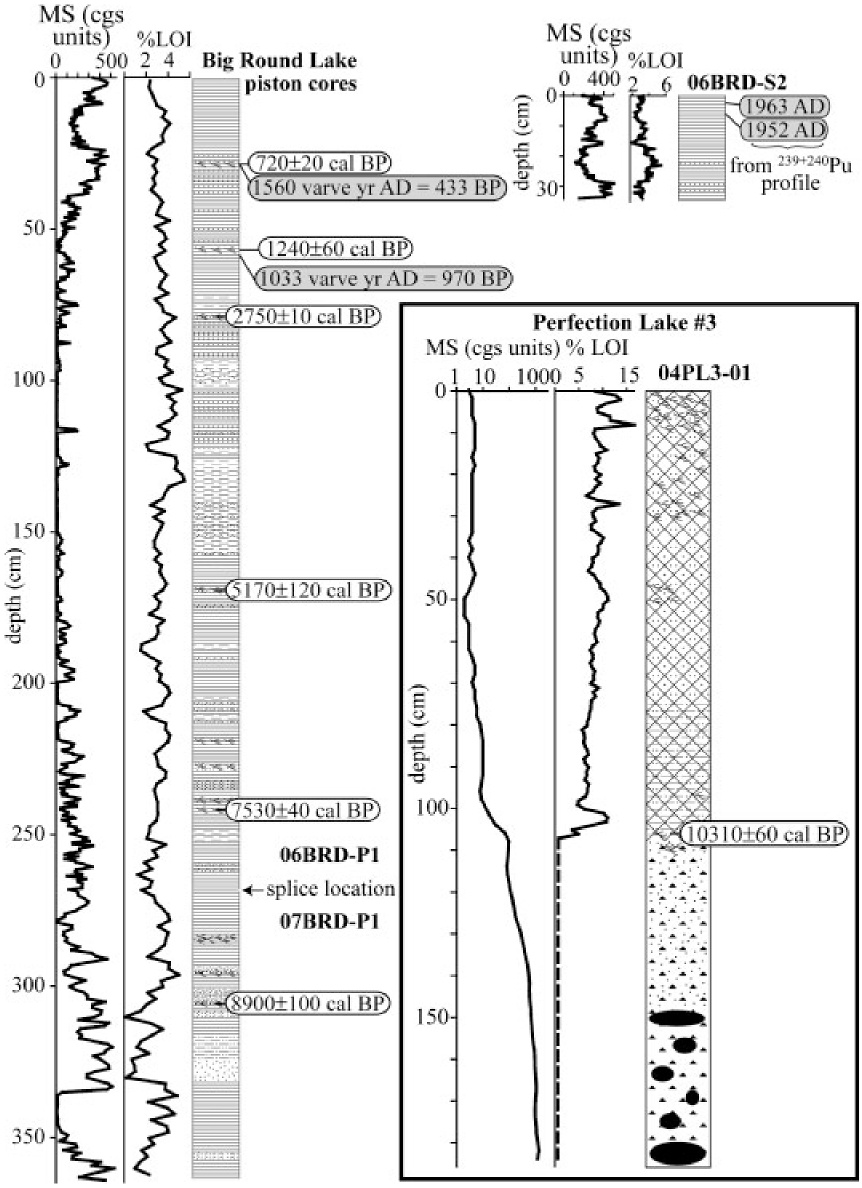

Figure 6 Core logs from Perfection Lake #3 and Big Round Lake, with age controls. See Fig. 3 for key

(07BRD-P1; 36.20 m depth; 69° 51.910′ N, 68° 51.484′ W) is 379 cm long. These two cores were correlated using their MS profiles, and spliced to obtain a composite long-core record (Fig. 6). LOI was measured on 1 cm thick subsamples every other centimetre. The surface core (06BRD-S2; 36.27 m depth; 69° 51.911′ N, 68° 51.571′ W) is 34 cm long (Fig. 6). LOI was measured every 0.5 cm on the surface core. A chronology was constructed for this core site by fitting a polynomial through ages provided by a $^{239+240}$Pu profile and varve counting in the surface core (Thomas and Briner, 2009) and six ^{14}C ages on terrestrial and aquatic macrofossils in the long cores (Table 2 and Fig. 4(c)). Where ages derived from the varve chronology overlap with ^{14}C ages, the calibrated ^{14}C ages at 1σ uncertainty are ca. 300 years older than the varve-based ages. This is probably because macrofossils do not grow *in situ* at this core site, but instead are carried there by high-energy events, and may have remained on the landscape or the lake bottom for some time before entrainment and re-deposition. We do not correct the age model for this offset between calibrated radiocarbon and varve ages, as we do not know the offset through the entire core. On the millennial timescales that we are concerned about for this study, this minor offset probably does not dramatically affect the age–depth model.

Varves have been identified in the upper 58 cm of these sediments (to AD 970; Thomas and Briner, 2009). Laminations similar to those identified as varves in the upper 58 cm appear at intervals throughout the record: 372–330 cm (10 190–9490 cal. a BP), 315–307 cm (9180–9000 cal. a BP), 290–251 cm (8590–7540 cal. a BP), 249–240 cm (7490–7220 cal. a BP), 225–210 cm (6770–6310 cal. a BP), 205–160 cm (6150–4700 cal. a BP) and 70–58 cm (1840–980 cal. a BP). Similarly, MS is high in the early Holocene (372–290 cm; 10 190–8590 cal. a BP), with an extreme low ~345–330 cm (9770–9490 cal. a BP), and is followed by a gradual decline until the middle Holocene (175 cm, 5190 cal. a BP), when the record reaches near-zero values and remains there, with a few small peaks, until the late Holocene (80 cm, 2140 cal. a BP). MS increases again during the late Holocene, with peaks 30–20 cm (700–440 cal. a BP) and 10–0 cm (180 cal. a BP to present).

Interpretation of glacier extent in the Big Round Lake catchment

The varve-like laminations in early and middle Holocene sediments from Big Round Lake likely result from similar

DOI: 10.1002/jqs

processes that deposited the varves in Big Round Lake surface sediments. These processes include annual variations in glacier melt, glacier sediment delivery to the lake and seasonal lake ice cover (Hodder *et al.*, 2007; Thomas and Briner, 2009). Deposition of these laminations therefore requires that the Kuuktannaq Glacier be present. This record has multiple intervals with varve-like laminations throughout the early Holocene (ca. 10–5 ka), while the middle Holocene (ca. 5–2 ka) lacks these laminations, suggesting that the Kuuktannaq Glacier was more extensive during the early and late Holocene than the middle Holocene. The MS record supports this lamination-based interpretation: MS is high in the early Holocene, when glacially derived sediment was deposited in Big Round Lake, and low in the mid–late Holocene (ca. 6–2 ka), when varve-like laminations were not as prevalent. This record suggests that a glacier likely was present in Big Round Lake's catchment at least from ca. 10–6 ka and from ca. 2 ka to the present.

Peep Lake

Peep Lake (informal name) is a small (0.02 km^2) kettle lake that lies in the hummocky landscape in Kuuktannaq Valley (Fig. 2(c)). Peep Lake has no defined inflow stream and no glacial input, and a small, ephemeral outflow. The centre of the lake basin, where a percussion core was collected, is 4.18 m deep.

Core 06PEEP-P1 is 64 cm long (69° 51.163′ N, 68° 40.103′ W; Table 1 and Fig. 7). The upper 33 cm are massive organic-rich lacustrine sediment with aquatic macrofossil-rich layers at 1 cm and 14–20 cm. Aquatic macrofossils from two of these layers were radiocarbon dated (Table 2). Below 33 cm, 06PEEP-P1 is composed of silty organic-rich sediment with millimetre-scale sand layers every 5–10 cm. A 2 cm thick sand layer at the bottom of the core contains aquatic macrofossils that yielded a basal radiocarbon age of 10 400 ± 110 cal. a BP (Table 2). MS and LOI corroborate the sedimentology of 06PEEP-P1: MS is high in the sand and silt and low in the organic-rich sediment, and LOI is low in the siltier sediment from 33–64 cm, but high (up to 24% where there are macrofossils) in the organic-rich sediment from 0 to 33 cm (Fig. 7).

Interpretation of glaciation based on Peep Lake sediments

The Peep Lake record constrains the timing of regional deglaciation with a basal age of 10 400 ± 100 cal. a BP. Peep Lake has an extremely low sedimentation rate throughout the

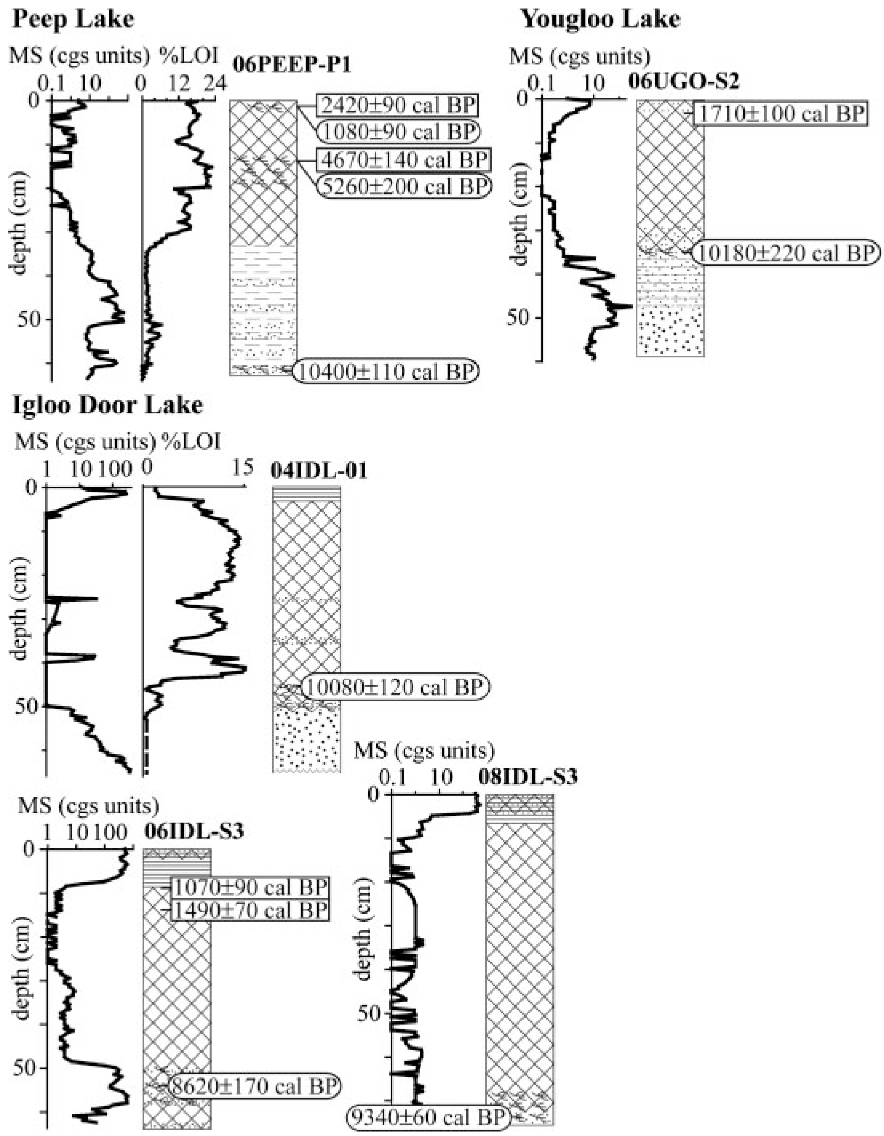

Figure 7 Core logs from Peep, Yougloo and Igloo Door lakes, with age controls. See Fig. 3 for key

Holocene (<0.001 cm a^{-1}, Fig. 4(d)) and was likely isolated from glaciers during this time. The intermittent sand layers deposited throughout the early Holocene were probably derived from catchment slopes during strong snow melt or rain events, not from proglacial meltwater.

Igloo Door Lake

Igloo Door Lake (informal name, 0.9 km^2 area) lies on the hummocky landscape in Kuuktannaq Valley, so it has a complex outline and bathymetry (Fig. 2(c)). Igloo Door Lake currently receives meltwater from the Kuuktannaq Glacier and its catchment is 38 km^2. When this glacier is less extensive, Igloo Door Lake's catchment size drops to 4.6 km^2 and does not have any glacial input. We collected one long core and two surface cores from the basin closest to the main inflow.

Core 04IDL-01 is a 70 cm long core retrieved 320 m from the inflow delta (5.63 m depth; 69° 51.18′ N, 68° 41.461′ W; Table 1 and Fig. 7). Core 06IDL-S3 is a 63 cm long surface core retrieved 130 m from the inflow delta (6.35 m depth; 69° 51.138′ N, 68° 41.881′ W; Table 1 and Fig. 7). Core 08IDL-S3 is a 75 cm long surface core retrieved 270 m from the inflow delta (4.65 m depth; 69° 51.206′ N, 68° 41.946′ W; Table 1 and Fig. 7). The stratigraphy of these three cores is similar (Fig. 7): laminated silt (3–8 cm thick) capping organic-rich lacustrine sediment (48–65 cm thick). All three cores contain several intermittent sandy layers, some with aquatic macrofossils, at and near the base of the organic-rich sediment. Core 04IDL-01 penetrated 20 cm into coarse sand that was likely deposited during deglaciation. Humic acid extracts from bulk sediment at the base of the laminated silt at 8.5 cm depth in 06IDL-S3 yield a radiocarbon age of 1070 ± 90 cal. a BP (Table 2). Aquatic macrofossils from within the early Holocene sand layers were dated in each core, yielding ages of 10 080 ± 120 cal. a BP at 46.25 cm in 04IDL01 (4 cm above the basal sand), 8620 ± 170 cal. a BP at 55 cm in 06IDLS3 and 9340 ± 60 cal. a BP at 73.7 cm in 08IDLS3.

Interpretation of glacier extent in the Igloo Door Lake catchment

All three cores from Igloo Door Lake have very low sedimentation rates throughout the Holocene (0.005–0.008 cm a^{-1}). The upper 3–9 cm of each core is composed of a laminated silt unit. This silt unit was deposited when the Kuuktannaq Glacier advanced to its LIA margin and crossed a topographic threshold, causing silt-laden meltwater to be diverted into the Igloo Door Lake basin. A bulk-sediment humic acid radiocarbon age on organic-rich sediment at the lower silt contact in 06IDL-S3 provides a maximum age of the LIA advance of the Kuuktannaq Glacier of 1070 ± 90 cal. a BP. Because the Kuuktannaq Glacier retreated only ~250 m between AD 1960 and 2000 (Fig. 2(c)), glacial meltwater still reaches the Igloo Door Lake basin today and the silty inflow stream and lake water are visible in aerial photographs and satellite imagery. The lack of a moraine beyond the LIA moraine and the lack of any other silt units in Igloo Door Lake sediments indicate not only that the LIA was the most extensive advance of the Kuuktannaq Glacier since the late Pleistocene, but also there were no Holocene advances similar in size to the LIA advance.

Sediments deposited in Igloo Door Lake throughout the middle Holocene are massive and organic-rich. During the early Holocene (ca. 10–8 ka), however, several intervals of high MS and low LOI correspond to coarse sand layers within the organic-rich sediments. We interpret these sand layers as non-glacial, because they are much coarser and more intermittent that the silt units deposited during the late Holocene. Instead, these sand units are likely sourced from catchment hillslopes during strong snow melt or rain events, suggesting elevated hillslope instability from 10 to 8 ka.

Yougloo Lake

Yougloo Lake (informal name) is another threshold lake that lies on the hummocky Kuuktannaq Valley floor (Fig. 2(c)). This 2.7 km^2 lake is sinuous and elongate. The 15.0 km^2 catchment currently receives meltwater from the Kuuktannaq Glacier. When the Kuuktannaq Glacier is less extensive, the catchment decreases to 9.0 km^2 and receives input from two non-moraine-forming glaciers (Fig. 1(c)).

Surface core 06UGO-S2 is 60 cm long (8.40 m depth; 69° 49.851′ N, 68° 36.436′ W; Table 1 and Fig. 7). Organic-rich lacustrine sediment extends from the surface of this core to 37 cm. The base of the core is composed of diffusely laminated sand (37–49 cm) and massive, coarse sand (49–60 cm). As in Igloo Door and Peep lake sediments, there are several millimetre-scale sand layers near the base of the organic-rich sediment in Yougloo Lake. Macrofossils found at 36 cm, 1 cm above the base of the organic sediment, yielded a radiocarbon age of 10 180 ± 220 cal. a BP. The upper 2 cm in 06UGO-S2 contain more silt than the rest of the organic-rich unit, which is reflected by a slight increase in MS values. A bulk-sediment humic acid radiocarbon age from just below this silt-rich unit is 1710 ± 100 cal. a BP.

Interpretation of glacier extent in the Yougloo Lake catchment

The basal age from 06UGO-S2 provides another minimum constraint on deglaciation, at 10 180 ± 220 cal. a BP. After deglaciation, Yougloo Lake experiences extremely low sedimentation rates (0.004 cm a^{-1}) and probably had very little glacial input throughout the Holocene. Some time after 1710 ± 100 cal. a BP, however, Yougloo Lake began to receive meltwater from the Kuuktannaq Glacier, due to the LIA advance across a topographic threshold, much like in Igloo Door Lake. The lack of silty layers elsewhere in 06UGO-S2 indicates that the LIA was the most extensive advance of the Kuuktannaq Glacier since >10.2 ka. The coarse sand layers near the base of 06UGO-S2 are similar in appearance to those found near the base of cores from Peep and Igloo Door Lakes, and were likely derived from surrounding hillslopes during snow melt or rain events during the early Holocene, instead of from several extremely short-lived glacier advances into the catchment.

Holocene glacier history of Perfection and Kuuktannaq Valleys

Deglaciation and early Holocene

The history of Holocene alpine glaciation in the study area begins with the retreat of the Laurentide Ice Sheet. Basal radiocarbon ages from three different lakes provide minimum limiting ages for deglaciation. A basal age from Perfection Lake #3 indicates that deglaciation occurred at or before

10 310 ± 60 cal. a BP in the Perfection Valley. Basal ages from Yougloo and Peep lakes in the Kuuktannaq Valley constrain deglaciation to 10 180 ± 220 cal. a BP and 10 400 ± 110 cal. a BP, respectively. One additional radiocarbon age from 4 cm above deglacial sand in Igloo Door Lake is 10 080 ± 120 cal. a BP. Taken together, these ages suggest that the mountain valleys between Inugsuin and McBeth fiords most likely deglaciated around 10.5 ka. That general timing of deglaciation agrees with constraints from the adjacent fiords, where cosmogenic ^{10}Be ages constrain deglaciation of outer McBeth Fiord to 10.8 ± 0.5 ka, and outer Clyde Inlet to 11.0 ± 0.5 ka (ages originally reported by Briner *et al.*, 2006b, are updated according to revised ^{10}Be production rates (Balco *et al.*, 2009)). In addition, radiocarbon ages from Clyde Inlet suggest that Laurentide ice retreated through the central portion of the fiord by 9.4 cal ka BP, and reached the fiord head by 9.2 cal ka BP (Briner *et al.*, 2007).

Alpine glacier moraines that pre-date Neoglaciation are found at several sites across Baffin Island (Briner *et al.*, 2009). One such moraine exists in the Perfection Valley floor and dams Perfection Lake #3 (Fig. 2(a)). The basal age in Perfection Lake #3 therefore also provides a minimum age for the deposition of this moraine at 10 310 ± 60 cal. a BP. The standstill or advance of this local glacier must have occurred shortly following the retreat of the Laurentide Ice Sheet from the study valleys. After this 10.3 ka advance, there is no evidence for any glacier advance more extensive than the LIA maximum position, including during the Cockburn Substage (9.6–8 ka), which is believed to be a period when some alpine glaciers on Baffin Island reached Holocene maximum positions (Briner *et al.*, 2009).

In Big Round Lake, sediments are most likely varved during several intervals in the early and middle Holocene. Because the lamination characteristics are similar to those in the top of the sediment sequence, which have been verified to be varves (Thomas and Briner, 2009), we infer that varved sediments were deposited in the early Holocene and that Big Round Lake was in a proglacial environment similar to today's. An alternative interpretation is that these laminations result from processes other than glacier activity, including fluvial and colluvial sediment delivery to the lake and seasonal freeze–thaw cycles. However, consistently high sedimentation rates throughout the Holocene and the similarity between early and late Holocene laminations lead us to conclude that these laminations are most likely glacially derived.

The threshold lakes (Igloo Door and Yougloo lakes) that record the Little Ice Age advance into their catchments contain organic-rich sediment interrupted by sandy layers in the early Holocene, but these sand layers are coarse and discontinuous, unlike the laminated silt units found in the surface sediments. Peep Lake, which has been isolated from glacial meltwater since deglaciation, also has sand layers in early Holocene sediments. This suggests that these sand layers in the early Holocene intervals of Igloo Door, Yougloo and Peep lakes are likely derived from non-glacial processes, such as runoff from adjacent hillslopes during snow melt or rain events. Although the threshold lakes indicate that the Kuuktannaq Glacier achieved its most extensive position since deglaciation during the Little Ice Age, varved sediments in Big Round Lake suggest that the Kuuktannaq Glacier likely existed during the early Holocene.

Middle Holocene

Sediments of middle Holocene age from proglacial lakes Longspur and Big Round are dominantly minerogenic. Laminated silt and sand at regular intervals in Longspur Lake, combined with relatively high sedimentation rates ($\sim$0.1 cm a^{-1}), suggest consistent input of minerogenic sediments from when the record begins ca. 9.2 ka through the middle Holocene. In contrast to Longspur Lake, which currently receives meltwater directly from five glaciers, Perfection Lake #3 receives meltwater directly from only one small, non-moraine-forming glacier, and contains organic-rich sediment deposited at much lower sedimentation rates ($\sim$0.01 cm a^{-1}) throughout the Holocene. If inflow to Longspur Lake was composed of less glacial meltwater, the sediments in Longspur Lake might be more organic, like the sediments in Perfection Lake #3. The juxtaposition of the two lakes in similar settings with contrasting sediment composition and rates of deposition suggest that glaciers may have persisted in the Longspur Lake catchment throughout the middle Holocene. Alternatively, the large, steep catchment of Longspur Lake may serve as a source for non-glacial minerogenic sediment to the lake, and therefore fluvial and colluvial processes could result in the strong minerogenic signal seen in Longspur Lake sediments. Perfection Lake #3, however, also has a steep catchment that would serve as a supply of fluvial and colluvial sediments, but the sediments from Perfection Lake #3 are predominantly organic. It is therefore likely that glaciers played a role in the deposition of sediment in Longspur Lake throughout the Holocene.

In Big Round Lake, the sedimentation rate is even higher than in Longspur Lake and the sediments are similarly minerogenic and even periodically varved. There is one portion in the Big Round Lake sediment sequence between ca. 6 and 2 ka, however, where MS drops to zero and the sediments are the least laminated and most organic in the entire sequence. Thus the period during the Holocene that most likely has minimum glacier extent is between ca. 6 and 2 ka.

Late Holocene

Although the maximum extent of alpine glaciers on Baffin Island occurred during the Little Ice Age, there is scattered evidence for the onset of Neoglaciation well before the Little Ice Age (Briner *et al.*, 2009). A significant shift in sediment grain size in Longspur Lake core 06PL4-P1 from the shallow core site might indicate a lake level change and thus the timing of moraine emplacement at the lake outlet ca. 3 ka. In Big Round Lake, sediments become varved again, and MS begins to increase, ca. 2140 cal. a BP (Fig. 6). Combined, the sediment changes in both lakes indicate that glaciers likely advanced to larger states ca. 3–2 ka.

As mentioned above, the maximum extent of glaciers in the Holocene occurred during the Little Ice Age. The threshold lakes (Igloo Door and Yougloo lakes), with basal ages of >10 ka, only contain glacier-derived silty sediments during the Little Ice Age. The lower contact of the silt is difficult to date owing to a lack of macrofossils and very low sedimentation rates, however, and only two bulk-sediment humic acid ages constrain the timing of when the Igloo Door and Yougloo lake basins were breached by the Kuuktannaq Glacier (1070 ± 90 cal. a BP and 1770 ± 70 cal. a BP, respectively). Elsewhere on Baffin Island bulk-sediment humic acid ages are 200–700 years older than aquatic macrofossil ages (Wolfe *et al.*, 2004); thus the Kuuktannaq Glacier likely breached these lake basins well after 1070 ± 90 cal. a BP or 1770 ± 70 cal. a BP. In AD 1960 the Kuuktannaq Glacier had retreated only a very minor distance from its LIA maximum position (Fig. 2(c)). Since AD 1960, the glacier has retreated 250 m, and the signal of silt input to Igloo Door and Yougloo lakes is diluted in the uppermost sediments by organic sediment deposition. Thus, in the Kuuktannaq Valley, the Little Ice Age maximum likely lasted well into the 20th century. The ~30 cm thick sand layer in Longspur Lake core 04PL4-02 is interpreted to represent moraine-front mass wasting from the glacier only ~700 m from the core site during the peak of the Little Ice Age. Although not precisely dated, the sandy unit was probably deposited between ca. AD 1500 and ca. 1800.

Holocene glacial and climate history of northeastern Baffin Island

Proxy records of Holocene climate change from northeastern Baffin Island and the broader Baffin Bay region provide climatic context for the history of Holocene glaciation in the study valleys. High boreal summer insolation led to a period of warmer-than-present conditions that are well expressed in most proxy records; however, the timing of maximum warmth differs. Chironomid-inferred summer temperatures from lakes on northeastern Baffin Island and the melt-layer record from the Agassiz Ice Cap define a period between ca. 10.5 and ca. 7 ka with peak summer warmth that was perhaps ~5°C warmer than today (Fisher *et al.*, 1995; Briner *et al.*, 2006a; Axford *et al.*, 2009; Fig. 8). Other records, like the $\delta^{18}O$ record from the Agassiz Ice Cap, show a broader period of warmth between ca. 9 and ca. 3 ka (Fisher *et al.*, 1995; Kaufman *et al.*, 2004). In addition, the peak in abundance of radiocarbon-dated thermophilous molluscs from northeastern Baffin Island occurred between 9.5 and 7.5 ka, and then remained elevated until 3.5 ka, indicating that surface ocean water between 9.5 and 3.5 ka was warmer than today (Dyke *et al.*, 1996a). The discrepancy in early *versus* middle Holocene warmth may lie in what the proxy records are recording. Seasonality was high in the early Holocene because of dramatic seasonal differences in solar insolation (Berger and Loutre, 1991). The presence of the shrinking Laurentide Ice Sheet also forced hot summers to remain short (Kaplan and Wolfe, 2006). Because seasonality was highest in the early Holocene, those proxies that respond to peak summer warmth (e.g. Agassiz Ice Cap melt layers) may show maximum temperatures in the early Holocene, whereas proxies that show mean annual warmth (e.g. Agassiz Ice Cap $\delta^{18}O$) reveal a broader period of warmth spanning the middle Holocene.

The sediment records from proglacial lakes reported here indicate that glaciers in their catchments most likely survived the early Holocene thermal maximum and were most reduced between ca. 6 and ca. 3 ka. This is an unexpected finding because summer solar insolation was highest in the early Holocene and we therefore hypothesise that this would be the interval of smallest glacier extent. If glacier extent was dominated by summer ablation, then glaciers should have been absent or most reduced during the early Holocene, perhaps between ca. 10 and ca. 7 ka. Although summer insolation was higher than present in the early Holocene, seasonality was enhanced. Summers were likely warmer than today, but also were shorter, due to insolation and the presence of the Laurentide Ice Sheet (Berger and Loutre, 1991; Kaplan and Wolfe, 2006), and a short ablation season would have resulted in less overall glacier melt. Another explanation for why alpine glaciers may have persisted during this interval of enhanced warmth is increased precipitation. Although proxy reconstructions for precipitation are lacking from this region, warmer surface ocean waters would likely have led to increased precipitation, and if some of it fell during the long arctic accumulation season then winter snowfall may have counteracted the elevated summer ablation. Increased minerogenic deposition in the early Holocene in non-glacial lake sediment sequences indicates that hillslope erosion was higher during this interval; perhaps this increased deposition of non-glacial minerogenic sediments indicates increased precipitation. Thus, perhaps elevated winter accumulation, in combination with short ablation seasons, led to the survival of glaciers during the early Holocene. Furthermore, it is

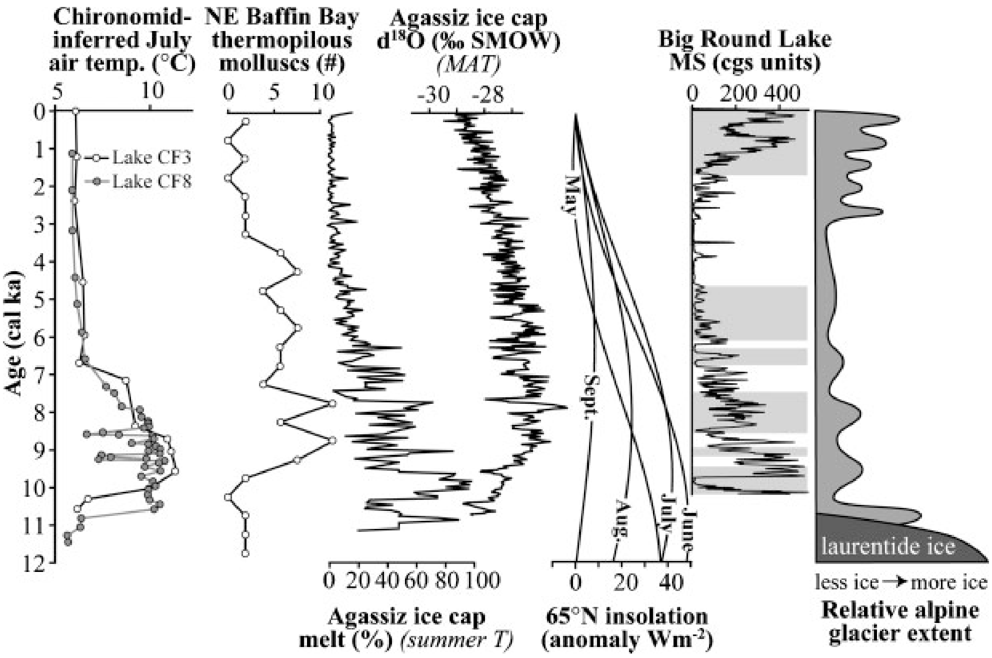

Figure 8 Big Round Lake magnetic susceptibility, plotted by age, and a Holocene glacier time–distance diagram for northeastern Baffin Island inferred from this study compared to regional climate records. Grey bars indicate periods of laminated couplet deposition in Big Round Lake. MAT, mean annual temperature. Chironomid-inferred July air temperature from Briner *et al.* (2006a; Lake CF3) and Axford *et al.* (2009; Lake CF8). NE Baffin Bay molluscs from Dyke *et al.* (1996a). Agassiz ice cap data from Fisher *et al.* (1995). Solar insolation data from Berger and Loutre (1991)

DOI: 10.1002/jqs

possible that glaciers were most reduced in the middle Holocene as this period may have had enhanced summer ablation, and decreased winter accumulation as surface–ocean waters began to cool (Dyke *et al.*, 1996a). Regardless, all proxy climate records show cooling in the late Holocene, and this seems to have led to distinct Neoglaciation evident in moraine records from across Baffin Island (Briner *et al.*, 2009) and in lake sediments in the Perfection and Kuuktannaq valleys.

Holocene glaciation in the Arctic

As was generally the case across Baffin Island, alpine glaciers in the study area reached their maximum late Holocene extent during the LIA (Miller *et al.*, 2005; Briner *et al.*, 2009). In a few areas, lichenometric results from pre-LIA moraine segments suggest that Neoglaciation initiated ca. 3.5–2.5 ka (e.g., Davis, 1985). Thus, although most alpine glaciers studied on Baffin Island approached their Neoglacial maxima as early as ca. 3.5 ka, glaciers were most extensive during the LIA. The general trend of alpine glaciers reaching their Neoglacial maxima during the LIA exists across the Arctic with very few exceptions (Kelly, 1980; Calkin, 1988; Mangerud and Landvik, 2007). Several valleys in northern Alaska contain pre-LIA moraines (Calkin, 1988; Young *et al.*, 2009), and moraines along some sectors of the Greenland Ice Sheet were apparently deposited during Neoglaciation prior to the LIA (Kelly, 1980; Bennike and Sparrenbom, 2007). However, because in most cases glaciers reached their largest Holocene extent during the LIA, information on pre-LIA ice extent is extremely sparse. Additional records from proglacial lake basins will help constrain information on smaller-than-present glaciers in the Arctic.

Conclusions

This study helps to address whether mountain glaciers and small mountain ice caps, which account for the majority of ice on Baffin Island, and a significant portion of sea-level rise (Abdalati *et al.*, 2004), were present in the early and middle Holocene. Although it has been documented that small ice caps on northern Baffin Island disappeared during the middle Holocene, and the Penny and the Barnes Ice Caps were present throughout the Holocene (Hooke and Clausen, 1982; Fisher *et al.*, 1998; Anderson *et al.*, 2008), there is very little knowledge about the history of medium-sized ice bodies in the eastern Canadian Arctic through the Holocene.

The moraine record in Perfection and Kuuktannaq valleys, dated by ice-marginal lake sediments, reveals glacier maxima occurring immediately prior to 10.3 ka and during the LIA. However, proglacial lacustrine sediments spanning the Holocene suggest that alpine glaciers were not absent between these moraine-forming periods, but rather may have persisted throughout the Holocene. Periods of varve formation and magnetic susceptibility in Big Round Lake suggest that glaciers were at least present in the early and late Holocene. Interestingly, the minimum glacier extent seems to have occurred between ca. 6 and ca. 3 ka, not in the early Holocene when regional proxy records reveal summer temperatures several degrees warmer than present. The survival of glaciers during the early Holocene Thermal Maximum perhaps stemmed from an ablation season that was shorter, albeit warmer, and an accumulation season that was longer, than at present. In contrast, the balance between winter precipitation and summer ablation may have been most negative in the middle Holocene. In any case, decreasing Boreal summer insolation and Baffin Bay surface temperatures led to Neoglaciation beginning ca. 3–2 ka and a subsequent peak of glaciation during the LIA. Additional records from proglacial lakes combined with proxy reconstructions of precipitation that span the Holocene would greatly improve reconstructions of Holocene glaciation in the Arctic, and hence knowledge of alpine glacier sensitivity to climate change.

Acknowledgements We are indebted to Jamesee Qillaq, Jason Hainnu and the Inuit of Clyde River for their logistical support. Aaron Bini, Steve DeVogel, Neal Michelutti, James R. Noble and Benjamin Schupack were also indispensable in the field. Thanks to Buffalo Ultrasound, Michael Ketterer, James R. Noble, Monica Ridgeway, Andrew Smith and John Stadler for their help in sample analysis and preparation. Whitney Autin graciously provided access to the particle size analyser. We thank Mike Kaplan and Atle Nesje for comments that strengthened the manuscript. This research was supported by the National Science Foundation, Arctic System Sciences program (ARC-0455024); we appreciate the licensing and logistical support provided by the Nunavut Research Institute and the National Science Foundation (VECO Polar Resources). The Geological Society of America partially supported this research in the form of a student research grant to EKT. The University at Buffalo Graduate Student Union and the Mark Diamond Research Fund partially supported this research in the form of a student research grant to JSS. EKT was supported by an NSF Graduate Research Fellowship.

References

Abbot MB, Stafford TWJ. 1996. Radiocarbon geochemistry of modern and ancient arctic lake systems, Baffin Island, Canada. *Quaternary Research* **45**: 300–311.

Abdalati W, Krabill W, Frederick E, Manizade S, Martin C, Sonntag J, Swift R, Thomas R, Yungel J, Koerner R. 2004. Elevation changes of ice caps in the Canadian Arctic Archipelago. *Journal of Geophysical Research* **109**: F04007.

ACIA. 2005. *Arctic Climate Impacts Assessment*. Cambridge University Press: Cambridge, UK.

Anderson RK, Miller GH, Briner JP, Lifton NA, DeVogel SB. 2008. A millennial perspective on Arctic warming from ^{14}C in quartz and plants emerging from beneath ice caps. *Geophysical Research Letters* **35**: L01502.

Andrews JT, Ives JD. 1978. 'Cockburn' nomenclature and the Late Quaternary history of the eastern Canadian Arctic. *Arctic and Alpine Research* **10**: 617–633.

Axford Y, Briner JP, Miller GH, Francis DR. 2009. Paleoecological evidence for abrupt cold reversals during peak Holocene warmth on Baffin Island, Arctic Canada. *Quaternary Research* **71**: 142–149.

Balco G, Briner JP, Finkel RC, Rayburn J, Ridge JC, Schaefer JM. 2009. Regional beryllium-10 production rate calibration for late-glacial northeastern North America. *Quaternary Geochronology* **4**: 93–107.

Bennike O, Sparrenbom CJ. 2007. Dating of the Narssarssuaq stade in southern Greenland. *The Holocene* **17**: 279–282.

Berger A, Loutre MF. 1991. Insolation values for the climate of the last 10 million years. *Quaternary Science Reviews* **10**: 291–310.

Bini AC. 2008. *An early Holocene deglaciation chronology for Sam Ford Fiord, Baffin Island, Arctic Canada: an analog for presently-retreating Greenland outlet glaciers*. MS thesis, University at Buffalo, Buffalo, NY.

Briner JP, Miller GH, Davis PT, Finkel RC. 2005. Cosmogenic exposure dating in Arctic glacial landscapes: implications for the glacial history of Northeastern Baffin Island, Arctic Canada. *Canadian Journal of Earth Sciences* **42**: 67–84.

Briner JP, Michelutti N, Francis DR, Miller GH, Axford Y, Wooller MJ, Wolfe AP. 2006a. A multi-proxy lacustrine record of Holocene climate change on northeastern Baffin Island. *Quaternary Research* **65**: 431–442.

Briner JP, Miller GH, Davis PT, Finkel RC. 2006b. Cosmogenic radionuclides from fiord landscapes support differential erosion by overriding ice sheets. *Geological Society of America Bulletin* **118**: 406–420.

Briner JP, Overeem I, Miller GH, Finkel R. 2007. The deglaciation of Clyde Inlet, northeastern Baffin Island, Arctic Canada. *Journal of Quaternary Science* **22**: 223–232.

Briner JP, Davis PT, Miller GH. 2009. Latest Pleistocene and Holocene glaciation of Baffin Island: key patterns and chronologies. *Quaternary Science Reviews* (in press).

Calkin PE. 1988. Holocene glaciation of Alaska (and adjoining Yukon Territory, Canada). *Quaternary Science Reviews* **7**: 159–184.

Chen H-W, Lee T, Ku T-L, Das JP. 2008. Production ratio of nuclear fallout $^{137}Cs/^{135}Cs$. *Chinese Journal of Physics* **46**: 560–569.

Crowley TJ. 2000. Causes of climate change over the past 1000 years. *Science* **289**: 270–277.

Davis PT. 1985. Neoglacial moraines on Baffin Island. In *Quaternary Environments: Eastern Canadian Arctic, Baffin Bay and Western Greenland*, Andrews JT (ed.). Allen & Unwin: Boston, MA; 682–718.

Davis PT, Briner JP, Coulthard RD, Finkel RC, Miller GH. 2006. Preservation of arctic landscapes overridden by cold-based ice sheets. *Quaternary Research* **65**: 156–163.

Dowdeswell EK, Dowdeswell JA, Cawkwell F. 2007. On the glaciers of Bylot Island, Nunavut, Arctic Canada. *Arctic, Antarctic and Alpine Research* **39**: 402–411.

Dyke AS, Dale JE, McNeely RN. 1996a. Marine molluscs as indicators of environmental change in glaciated North America and Greenland during the last 18000 years. *Géographie Physique et Quaternaire* **50**: 125–184.

Dyke AS, Hooper J, Savelle JM. 1996b. A history of sea ice in the Canadian Arctic Archipelago based on postglacial remains of the bowhead whale (*Balaena mysticetus*). *Arctic* **49**: 235–255.

Environment Canada, National Climate Archive. 2007. http://climate.-weatheroffice.ec.gc.ca [1 October 2007].

Fisher DA, Koerner RM, Reeh N. 1995. Holocene climatic records from Agassiz Ice Cap, Ellesmere Island, NWT, Canada. *The Holocene* **5**: 19–24.

Fisher DA, Koerner RM, Bourgeois JC, Zielinski G, Wake C, Hammer CU, Clausen HB, Gundestrup N, Johnsen S, Goto-Azuma K, Hondoh T, Blake E, Gerasimoff M. 1998. Penny Ice Cap cores, Baffin Island, Canada, and the Wisconsin Foxe Dome connection: two states of Hudson Bay ice cover. *Science* **279**: 692–695.

Francus P, Asikainen C. 2001. Sub-sampling unconsolidated sediments: a solution for the preparation of undisturbed thin-sections from clay-rich sediments. *Journal of Paleolimnology* **26**: 323–326.

Gillett NP, Stone DA, Stott PA, Nozawa T, Karpechko AY, Hegerl GC, Wehner MF, Jones PD. 2008. Attribution of polar warming to human influence. *Nature Geosciences* **1**: 750–753.

Hodder KR, Gilbert R, Desloges JR. 2007. Glaciolacustrine varved sediment as an alpine hydroclimatic proxy. *Journal of Paleolimnology* **38**: 365–394.

Hooke R Le B, Clausen HB. 1982. Wisconsin and Holocene $\delta^{18}O$ variations, Barnes Ice Cap, Canada. *Geological Society of America Bulletin* **93**: 784–789.

IPCC. 2007. Summary for Policymakers. In *Climate Change 2007: The Physical Science Basis. Contribution of Working Group I to the Fourth Assessment Report of the Intergovernmental Panel on Climate Change*. Cambridge University Press: Cambridge, UK; 2–18.

Kaplan MR, Wolfe AP. 2006. Spatial and temporal variability of Holocene temperature in the North Atlantic region. *Quaternary Research* **65**: 223–231.

Kaufman DS, Ager TA, Anderson NJ, Anderson PM, Andrews JT, Bartlein PJ, Brubaker LB, Coats LL, Cwynar LC, Duvall ML, Dyke AS, Edwards ME, Eisner WR, Gajewski K, Geirsdóttir A, Hu FS, Jennings AE, Kaplan MR, Kerwin MW, Lozhkin AV, MacDonald GM, Miller GH, Mock CJ, Oswald WW, Otto-Bliesner BL, Porinchu DF, Rühland K, Smol JP, Steig EJ, Wolfe BB. 2004. Holocene thermal maximum in the western Arctic (0–180° W). *Quaternary Science Reviews* **23**: 529–560.

Kelly M. 1980. The status of the Neoglacial in western Greenland. *Rapport Grønlands Geologiske Undersøgelse* no. 96.

Ketterer ME, Hafer KM, Link CL, Kolwaite D, Wilson J, Mietelski JW. 2004. Resolving global versus local/regional Pu sources in the environment using sector ICP-MS. *Journal of Analytical Atomic Spectrometry* **19**: 241–245.

Lamoureux SF. 1994. Embedding unfrozen lake sediments for thin section preparation. *Journal of Paleolimnology* **10**: 141–146.

Lamoureux SF, Gilbert R. 2004. A 750-yr record of autumn snowfall and temperature variability and winter storminess recorded in the varved sediments of Bear Lake, Devon Island, Arctic Canada. *Quaternary Research* **61**: 134–137.

Mangerud J, Landvik JY. 2007. Younger Dryas cirque glaciers in western Spitsbergen: smaller than during the Little Ice Age. *Boreas* **36**: 278–285.

Meier MF, Dyurgerov MB, Rick UK, O'Neel S, Pfeffer WT, Anderson RS, Anderson SP, Glazovsky AF. 2007. Glacier dominate eustatic sea-level rise in the 21st century. *Science* **317**: 1064–1067.

Michelutti N, Wolfe AP, Vinebrooke RD, Rivard B, Briner JP. 2005. Recent primary production increases in arctic lakes. *Geophysical Research Letters* **32**: L19715.

Miller GH. 1973. Variations in lichen growth from direct measurements: preliminary curves for *Alectoria minuscula* from eastern Baffin Island, N.W.T. Canada. *Arctic and Alpine Research* **5**: 333–339.

Miller GH, Mode WN, Wolfe AP, Sauer PE, Bennike O, Forman SL, Short SK, Stafford TW Jr. 1999. Stratified interglacial lacustrine sediment from Baffin Island, Arctic Canada: chronology and paleoenvironmental implications. *Quaternary Science Reviews* **18**: 789–810.

Miller GH, Wolfe AP, Briner JP, Sauer PE, Nesje A. 2005. Holocene glaciation and climate evolution of Baffin Island, Arctic Canada. *Quaternary Science Reviews* **24**: 1703–1721.

Moore JJ, Hughen KA, Miller GH, Overpeck JT. 2001. Little Ice Age recorded in summer temperature reconstruction from varved sediments of Donard Lake, Baffin Island, Canada. *Journal of Paleolimnology* **25**: 503–517.

Nesje A. 1992. A piston corer for lacustrine and marine sediments. *Arctic and Alpine Research* **24**: 257–259.

Otto-Bliesner BL, Brady EC, Clauzet G, Tomas R, Levis S, Kothavala Z. 2006. Glacial Maximum and Holocene Climate in CCSM3. *Journal of Climate* **19**: 2526–2544.

Paul F, Kääb A. 2005. Perspectives on the production of a glacier inventory from multispectral satellite data in Arctic Canada: Cumberland Peninsula, Baffin Island. *Annals of Glaciology* **42**: 59–66.

Serreze MC, Holland MM, Stroeve J. 2007. Perspectives on the Arctic's shrinking sea-ice cover. *Science* **315**: 1533–1536.

Szymanski JS. 2008. *Holocene glaciation of Perfection Valley, Baffin Island, Arctic Canada*. MS thesis, University at Buffalo, Buffalo, NY.

Thomas EK, Briner JP. 2009. Climate of the past millennium inferred from varved proglacial lake sediments on northeast Baffin Island, Arctic Canada. *Journal of Paleolimnology* **41**: 209–224.

Wolfe AP, Miller GH, Olsen CA, Forman SL, Doran PT, Holmgren SU. 2004. Geochronology of high latitude lake sediments. In *Long-Term Environmental Change in Arctic and Antarctic Lakes*, Pienitz R, Douglas MSV, Smol JP (eds). Kluwer: Dordrecht; 1–32.

Young NE, Briner JP, Kaufman DS. 2009. Late Pleistocene and Holocene glaciation of the Fish Lake valley, northeastern Alaska Range, Alaska. *Journal of Quaternary Science* (in press). DOI: 10.1002/jqs.1279